

term on the left-hand side corresponding to the kinetic energy of the expanding fluid and the first term on the right-hand side to its gravitational potential energy, as we will show in Sect. 7.2. An illuminating account of Friedman's equation, its physical content and its solutions has been given by White, whose presentation can be thoroughly recommended (White, 1990). The pair of equations (7.1) and (7.2) incorporate the First Law of Thermodynamics in its full relativistic form as can be appreciated from the following analysis. We write the first law in the usual form

$$dU = -p dV . \quad (7.3)$$

We need to formulate the law so that it is applicable for relativistic and non-relativistic fluids and so we write the internal energy U as the sum of all the terms which can contribute to the total energy of the fluid in the relativistic sense. Thus, the total internal energy consists of the fluid's rest mass energy, its kinetic energy, its thermal energy and so on. If we write the sum of these energies as $\varepsilon_{\text{tot}} = \sum_i \varepsilon_i$, the internal energy is $\varepsilon_{\text{tot}} V$ and so, dividing (7.3) by dV , it follows that

$$\frac{d}{da} (\varepsilon_{\text{tot}} V) = -p \frac{dV}{da} . \quad (7.4)$$

Now, $V \propto a^3$ and so, differentiating, we find

$$\frac{d\varepsilon_{\text{tot}}}{da} + 3 \frac{(\varepsilon_{\text{tot}} + p)}{a} = 0 . \quad (7.5)$$

This result can be expressed in terms of the inertial mass density associated with the total energy $\varepsilon_{\text{tot}} = Qc^2$; this is the type of density q which should be included in (7.1) and (7.2). Therefore, (7.5) can also be written

$$\frac{dq}{da} + 3 \frac{\left(q + \frac{p}{c^2}\right)}{a} = 0 . \quad (7.6)$$

Let us show how (7.5) and (7.6) lead to a number of important results which we will use repeatedly in what follows. First of all, suppose the fluid is very 'cold' in the sense that $p \ll q_0 c^2$, where q_0 is its rest mass density. Then, setting $p = 0$ and $\varepsilon_0 = Nmc^2$, where N is the number density of particles of rest mass m , we find

$$\frac{dN}{da} + \frac{3N}{a} = 0 \quad \text{and so} \quad N = N_0 a^{-3} , \quad (7.7)$$

that is, the equation of conservation of mass for a gas of non-relativistic particles.

Next, the thermal pressure of non-relativistic matter can be included into (7.5). We will normally be dealing with monatomic gases or plasmas for which the thermal energy is $\varepsilon_{\text{th}} = \frac{3}{2} NkT$ and $p = NkT$. Then, substituting $\varepsilon_{\text{tot}} = \frac{3}{2} NkT + Nmc^2$ and $p = NkT$ into (7.5), we find

$$\begin{aligned} \frac{d}{da} \left(\frac{\left(\frac{3}{2} NkT + Nmc^2\right)}{a} + 3 \left(\frac{\frac{3}{2} NkT + Nmc^2}{a} \right) \right) &= 0 , \\ \frac{d(NkT)}{da} + \frac{5NkT}{a} &= 0 \quad \text{and so} \quad NkT = N_0 kT_0 a^{-5} . \end{aligned} \quad (7.8)$$

Since $N = N_0 a^{-3}$, we find the standard result for the adiabatic expansion of a monatomic gas with ratio of specific heats $\gamma = 5/3$, $T \propto a^{-2}$. More generally, if the ratio of specific heats of the gas is γ , the energy density is $\varepsilon_{\text{tot}} = NkT/(\gamma - 1) + Nmc^2$ and so the temperature changes as $T \propto a^{-3(\gamma-1)}$.

We can deduce another important result from the expression for a monatomic gas, $T \propto a^{-2}$. If we write $\varepsilon_{\text{th}} = \frac{1}{2} Nm \langle v^2 \rangle$, where $\langle v^2 \rangle$ is the mean square velocity of the particles of the gas, we find $\langle v^2 \rangle \propto a^{-2}$. Thus, the random velocities of the particles of the gas decrease as $v \propto a^{-1}$. This result applies equally to the random motions of galaxies relative to the mean Hubble flow, what are known as the *peculiar velocities* of galaxies, v_{pec} . Therefore, as the Universe expands, we expect the peculiar velocities of galaxies to decrease as $v_{\text{pec}} \propto a^{-1}$.

Finally, in the case of a gas of ultrarelativistic particles, or a gas of photons, we can write $p = \frac{1}{3} \varepsilon_{\text{tot}}$. Therefore, from (7.5),

$$\frac{d\varepsilon_{\text{tot}}}{da} + \frac{4\varepsilon_{\text{tot}}}{a} = 0 \quad \text{and so} \quad \varepsilon_{\text{tot}} \propto a^{-4} . \quad (7.9)$$

In the case of a gas of photons, $\varepsilon_{\text{rad}} = \sum Nhv$ and, since $N \propto a^{-3}$, we find $v \propto a^{-1}$. This is an alternative derivation of the relation between the scale factor a and the cosmological redshift z . If v_0 is the frequency of the photon at the present epoch and v_{em} its frequency when the scale factor was a , $v_{\text{em}}/v_0 = a^{-1}$ and hence, from the definition of (5.45),

$$z = \frac{v_{\text{em}}}{v_0} - 1 ; \quad a = \frac{1}{1+z} . \quad (7.10)$$

Let us now return to the analysis of (7.2). Differentiating this equation with respect to time and dividing through by \dot{a} , we find

$$\dot{a} = \frac{4\pi G a^2}{3} \frac{dq}{da} + \frac{8\pi G \varrho a}{3} + \frac{1}{3} \Lambda a . \quad (7.11)$$

Now, substituting the expression for dq/da from (7.6), we find

$$\dot{a} = -\frac{4\pi G a}{3} \left(\varrho + \frac{3p}{c^2} \right) + \frac{1}{3} \Lambda a , \quad (7.12)$$

that is, we recover (7.1). The purpose of these calculations has been to show how (7.1) and (7.2) correctly include the law of conservation of energy for both relativistic and non-relativistic gases.

Equation (7.1) has the form of a force equation, but, as we have shown, it contains implicitly the First Law of Thermodynamics as well. An equation of this form can be derived from Newtonian considerations, but it does not contain the pressure term $3p/c^2$. This pressure term can be considered a 'relativistic correction' to the inertial mass density, but it is unlike normal pressure forces which depend upon the gradient of the pressure and, for example, hold up the stars. The term $\varrho + (3p/c^2)$ can be thought of as playing the role of an *active gravitational mass density*.

The general solutions of (7.2) for expanding world models were discovered by Aleksander Aleksandrovich Friedman in two remarkable papers published in 1922 and 1924 (Friedman, 1922, 1924) (for translations, see the book *Cosmological Constants* (Bernstein and Feinberg, 1986)). In these papers, Friedman assumed that $\Lambda \neq 0$ and so it is appropriate to refer to the complete set of models with and without the Λ -term as the *Friedman world models*.

As we will discuss in Chaps. 8 and 15, there is now compelling evidence for a finite value of the cosmological constant Λ . It might therefore seem best to plunge straight into the full analysis of (7.1) and (7.2) with $\Lambda \neq 0$. Rather than do this, I will develop the models with and without a finite value of Λ in parallel in what follows. There are two reasons for not discarding the models with $\Lambda = 0$ immediately. The first is that the models with $\Lambda = 0$ often have simple analytic solutions which give insight into the behaviour of the cosmological models. The second reason is that the effects of the cosmological constant only become appreciable at late cosmological epochs and so for many purposes, particularly in the early Universe, we can confidently set the cosmological constant equal to zero.

7.2 The Standard Friedman World Models with $\Lambda = 0$

By *dust*, cosmologists mean a pressureless fluid and so we set $p = 0$ in the Friedman equations. In this section, the cosmological constant Λ is also set to zero. It is convenient to refer to the density of the fluid to its value at the present epoch ρ_0 and then, because of conservation of mass, $\rho = \rho_0 a^{-3}$. Therefore, (7.1) and (7.2) reduce to

$$\ddot{a} = -\frac{4\pi G \rho_0}{3a^2}; \quad \dot{a}^2 = \frac{8\pi G \rho_0}{3a} - \frac{c^2}{3a^2}. \quad (7.13)$$

7.2.1 The Newtonian Analogue of the Friedman World Models

In 1934, Milne and McCrea showed that relations of the form (7.13) can be derived using non-relativistic Newtonian dynamics (Milne and McCrea, 1934a,b). We will perform this calculation because the ideas implicit in the argument can be used to understand some of the problems which arise in the theory of galaxy formation. Consider a galaxy at distance x from the Earth and work out its deceleration due to the gravitational attraction of the matter inside the sphere of radius x centred on the Earth (Fig. 7.1). By Gauss's theorem, because of the spherical symmetry of the distribution of matter about the origin, we can replace that mass, $M = (4\pi/3)\rho x^3$, by a point mass at the centre of the sphere and so the deceleration of the galaxy is

$$m\ddot{x} = -\frac{G M m}{x^2} = -\frac{4\pi x \rho m}{3}. \quad (7.14)$$

The mass of the galaxy m cancels out on either side of the equation, showing that the deceleration refers to the sphere of matter as a whole rather than to any particular position in Fig. 7.1, an observer located on any galaxy anywhere in the Universe

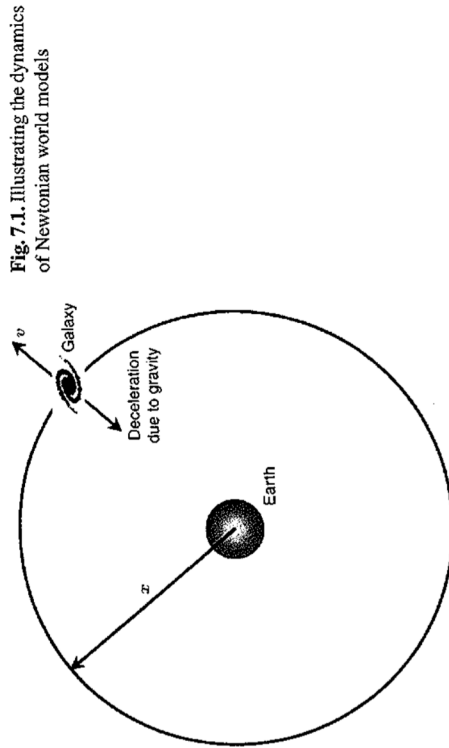


Fig. 7.1. Illustrating the dynamics of Newtonian world models

galaxy. We now replace x by the comoving radial distance coordinate r using the relation $x = ar$, and express the density in terms of its value at the present epoch, $\rho = \rho_0 a^{-3}$. Then,

$$\ddot{a} = -\frac{4\pi G \rho_0}{3a^2}, \quad (7.15)$$

which is identical to (7.1) for dust models with $\Lambda = 0$. Multiplying (7.15) by \dot{a} and integrating, we find

$$\dot{a}^2 = \frac{8\pi G \rho_0}{3a} + \text{constant}. \quad (7.16)$$

This result is identical to (7.2) if we identify the constant with $-c^2/3r^2$. This Newtonian calculation illustrates why we can identify the left-hand side of (7.2) with the kinetic energy of expansion of the fluid and the first term on the right-hand side with its gravitational potential energy.

The above analysis brings out a number of important features of the Friedman world models. First of all, there is an important flaw in the Newtonian argument in that we have applied Gauss's law to an infinite distribution of matter and ignored the issue of the boundary conditions at infinity. The argument works, however, because of the assumption of isotropy and homogeneity of the matter throughout the infinite Universe; local physics is also global physics. The same physics which defines the local behaviour of matter also defines its behaviour on the largest scales. For example, the curvature of space κ within one cubic metre is exactly the same as that on the scale of the Universe itself.

Furthermore, although we might appear to have placed the Earth in a preferred position in Fig. 7.1, an observer located on any galaxy anywhere in the Universe

would perform exactly the same calculation to estimate the deceleration of any other galaxy relative to the observer's galaxy. This is a result of the cosmological principle which asserts that all fundamental observers should observe the same large-scale features of the Universe at the same epoch. In other words, the Newtonian calculation applies for all observers who move in such a way that the Universe appears isotropic to them which is, by definition, for all fundamental observers.

Notice also that at no point in the argument did we ask over what physical scale the calculation was to be valid. For strictly uniform isotropic models, this calculation describes correctly the dynamics of the Universe on scales greater than the *horizon scale* which, for the moment, we can take to be $r = ct$, that is, the maximum distance between points which can be causally connected at the epoch t . The reason for this is the same as for the first two points: local physics is also global physics and so, if the Universe were set up in such a way that it had uniform density on scales far exceeding the horizon scale, the dynamics on these very large scales would be exactly the same as the local dynamics.

Friedman died of typhoid during the civil war in Leningrad in 1925 and did not live to see what have become the standard models of the Universe bear his name (see the biography by Tropp, Frenkel and Chernin (Tropp et al., 1993)). It is perhaps surprising that these papers did not attract more widespread interest at the time. This may have been partly due to a brief note published by Einstein in 1922 criticising some steps in Friedman's first paper (Einstein, 1922). In the following year, Einstein graciously acknowledged that his criticism was based upon an error in his own calculations and that Friedman's solution was indeed correct (Einstein, 1923). Georges Lemaître rediscovered Friedman's solutions in 1927 and brought Friedman's contributions to the wider notice of astronomers and cosmologists during the 1930s (Lemaître, 1927).

7.2.2 The Critical Density and the Density Parameter

It is convenient to express the density of the world models in terms of a *critical density* Ω_c which is defined to be

$$\Omega_c = (3H_0^2/8\pi G) = 1.88 \times 10^{-26} h^2 \text{ kg m}^{-3}. \quad (7.17)$$

Where Hubble's constant H_0 has been written $H_0 = 100 \text{ km s}^{-1} \text{ Mpc}^{-1}$ in view of uncertainty about its exact value.¹ Then, the actual density of the model at the present epoch Ω_0 can be referred to this value through a *density parameter* $\Omega_0 = \varrho_0/\varrho_c$. Thus, the density parameter is defined to be

$$\Omega_0 = \frac{\varrho_0}{\varrho_c} = \frac{8\pi G \varrho_0}{3H_0^2}. \quad (7.18)$$

The subscript 0 has been attached to Ω because the critical density ϱ_c changes with cosmic epoch, as does Ω . It is convenient to refer any cosmic density to ϱ_c .

¹ As will be discussed in Chaps. 8 and 15, Hubble's constant is now known to better than 10% accuracy. A value of $h = 0.7$ can be used with some confidence.

For example, we will often refer to the density parameter of baryons, Ω_B , or of visible matter, Ω_{vis} , or of dark matter, Ω_D , and so on; these are convenient ways of describing the relative importance of different contributions to Ω_0 .

The dynamical equations (7.13) therefore become

$$\ddot{a} = -\frac{\Omega_0 H_0^2}{2a^2}; \quad d^2 = \frac{\Omega_0 H_0^2}{a} - \frac{c^2}{\mathfrak{N}^2}. \quad (7.19)$$

Several important results can be deduced from these equations. If we set the quantities in the second equation of (7.19) equal to their values at the present epoch, $t = t_0$, $a = 1$ and $\dot{a} = H_0$, we find

$$\mathfrak{N} = \frac{c/H_0}{(\Omega_0 - 1)^{1/2}} \quad \text{and} \quad \kappa = \frac{(\Omega_0 - 1)}{(c/H_0)^2}. \quad (7.20)$$

This last result shows that there is a one-to-one relation between the density of the Universe Ω_0 and its spatial curvature κ , one of the most beautiful results of the Friedman world models with $\Lambda = 0$.

7.2.3 The Dynamics of the Friedman Models with $\Lambda = 0$

To understand the solutions of (7.19), we substitute (7.20) into (7.19) to find the following expression for \dot{a}

$$\dot{d}^2 = H_0^2 \left[\Omega_0 \left(\frac{1}{a} - 1 \right) + 1 \right]. \quad (7.21)$$

In the limit of large values of a , \dot{d}^2 tends to

$$\dot{d}^2 = H_0^2 (1 - \Omega_0). \quad (7.22)$$

Thus:

- The models having $\Omega_0 < 1$ have open, hyperbolic geometries and expand to $a = \infty$. They continue to expand with a finite velocity at $a = \infty$ with $\dot{a} = H_0(1 - \Omega_0)^{1/2}$.
- The models with $\Omega_0 > 1$ have closed, spherical geometry and stop expanding at some finite value of $a = a_{\max}$ – they have 'imaginary expansion rates' at infinity. They reach the maximum value of the scale factor after a time

$$t_{\max} = \frac{\pi \Omega_0}{2H_0(\Omega_0 - 1)^{3/2}}. \quad (7.23)$$

These models collapse to an infinite density after a finite time $t = 2t_{\max}$, an event sometimes referred to as the 'big crunch'.

- The model with $\Omega_0 = 1$ separates the open from the closed models and the collapsing models from those which expand forever. This model is often referred to as the *Einstein-de Sitter* or the *critical model*. The velocity of expansion tends

model. It is an interesting exercise to show why it is that, in the completely empty world model, the global geometry of the Universe is hyperbolic. The reason is that, in the empty model, the galaxies partaking in the universal expansion are undecelerated and any particular galaxy always has the same velocity relative to the same fundamental observer. Therefore, the cosmic times measured in different frames of reference are related by the standard Lorentz transform $t' = \gamma(t - vr/c^2)$ where $\gamma = (1 - v^2/c^2)^{-1/2}$. The key point is that the conditions of isotropy and homogeneity apply at constant cosmic time t' in the frames of reference of all fundamental observers. The Lorentz transform shows that this cannot be achieved in flat space but it is uniquely satisfied in hyperbolic space with $\kappa = -(H_0/c)^2$. A simple derivation of this result is given in the Appendix to this chapter. The general solutions of (7.21) are most conveniently written in parametric form. For $\Omega_0 > 1$,

$$a = \left(\frac{t}{t_0}\right)^{2/3} \quad \kappa = 0, \quad (7.24)$$

where the present age of the world model is $t_0 = (2/3)H_0^{-1}$.

Some solutions of (7.21) are displayed in Fig. 7.2 which shows the well-known relation between the dynamics and geometry of the Friedman world models with $\Lambda = 0$. The abscissa in Fig. 7.2 is in units of H_0^{-1} and so the slope of the relations at the present epoch, $a = 1$, is always 1. The present age of the Universe is given by the intersection of each curve with the line $a = 1$.

Another useful result is the function $a(t)$ for the empty world model, $\Omega_0 = 0$, $a(t) = H_0 t$, $\kappa = -(H_0/c)^2$. This model is sometimes referred to as the *Milne*

$$a = A(1 - \cos \theta) \quad t = B(\theta - \sin \theta), \quad (7.25)$$

$$A = \frac{\Omega_0}{2(\Omega_0 - 1)} \quad \text{and} \quad B = \frac{\Omega_0}{2H_0(\Omega_0 - 1)^{3/2}}. \quad (7.26)$$

For $\Omega_0 < 1$,

$$a = A(\cosh \phi - 1) \quad t = B(\sinh \phi - \phi), \quad (7.27)$$

$$A = \frac{\Omega_0}{2(1 - \Omega_0)} \quad \text{and} \quad B = \frac{\Omega_0}{2H_0(1 - \Omega_0)^{3/2}}. \quad (7.28)$$

All the models tend towards the dynamics of the critical model at early times but with a different constant, that is, for $\theta \ll 1$ and $\phi \ll 1$,

$$a = \Omega_0^{1/3} \left(\frac{3H_0 t}{2} \right)^{2/3}. \quad (7.29)$$

We will find these results useful in understanding the growth of small perturbations in the expanding Universe (Sect. 11.4.2).

7.3 Friedman Models with Non-Zero Cosmological Constant

The tortuous history of the cosmological constant Λ was told briefly in Chap. 1 and need not be repeated here. So far as the interpretation of the term is concerned, Einstein soon realised that the Λ -term would appear as a constant in his field equations quite independent of its cosmological significance (Einstein, 1919). In 1933, Lemaître suggested that the Λ -term could be interpreted in terms of a finite vacuum energy density (Lemaître, 1933). In his words:

Everything happens as though the energy in vacuo would be different from zero.

This insight foreshadows the present interpretation of the cosmological constant which associates it with *dark energy*, the nature of which is one of the great unsolved cosmological mysteries. Let us illustrate how this remarkable situation has come about.

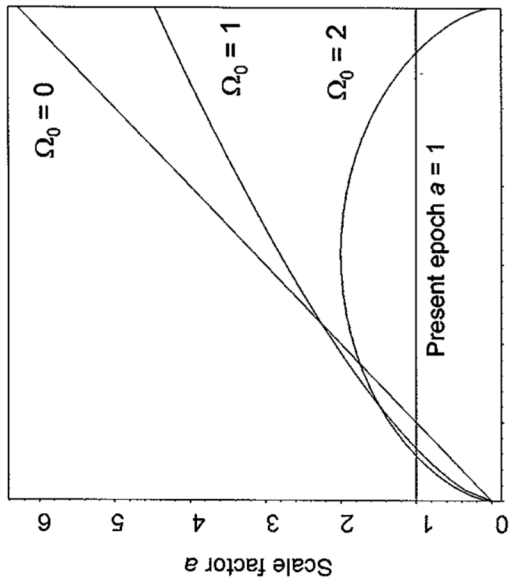


Fig. 7.2. The dynamics of the classical Friedman models with $\Omega_\Lambda = 0$ characterised by the density parameter $\Omega_0 = \rho_0/\rho_c$. If $\Omega_0 > 1$, the Universe collapses to $a = 0$ as shown; if $\Omega_0 < 1$, the Universe expands to infinity and has a finite velocity of expansion as a tends to infinity. In the case $\Omega_0 = 1$, $a = (t/t_0)^{2/3}$ where $t_0 = (2/3)H_0^{-1}$. The time axis is given in terms of the dimensionless time $H_0 t$. At the present epoch $a = 1$ and in this presentation, the three curves have the same slope of 1 at $a = 1$, corresponding to a fixed value of Hubble's constant at the present day. If t_0 is the present age of the Universe, then $H_0 t_0 = 1$ for $\Omega_0 = 0$, $H_0 t_0 = 2/3$ for $\Omega_0 = 1$ and $H_0 t_0 = 0.57$ for $\Omega_0 = 2$.

Press and Turner have described how a theoretical value of Λ can be estimated using simple concepts from quantum field theory (Carroll et al., 1992). In their approach, they perform a standard analysis to estimate the energy density of the vacuum fields by integrating to a maximum wavenumber k_{\max} at which the theory breaks down. They find

$$\dot{a} = -\frac{4\pi Ga}{3} \left(\varrho + \frac{3p}{c^2} \right) + \frac{1}{3}\Lambda a ; \quad (7.30)$$

$$\ddot{a}^2 = \frac{8\pi G\varrho a^2 - \frac{c^2}{3} + \frac{1}{3}\Lambda a^2}{a^2} . \quad (7.31)$$

Considering dust-filled universes as in Sect. 7.2, we set $3p/c^2 = 0$ and then (7.30) becomes

$$\ddot{a} = -\frac{4\pi Ga\varrho}{3} + \frac{1}{3}\Lambda a = -\frac{4\pi G\varrho_0}{3a^2} + \frac{1}{3}\Lambda a . \quad (7.32)$$

Inspection of (7.32) gives some insight into the physical meaning of the cosmological constant. Even in an empty universe, $\varrho = 0$, there is a net force acting on a test particle. If Λ is positive, the term may be thought of as the ‘repulsive force of a vacuum’, in the words of Zeldovich, the repulsion being relative to an absolute geometrical frame of reference (Zeldovich, 1968). There was no obvious interpretation of the Λ -term according to classical physics. There is, however, a natural interpretation in the context of quantum field theory.

A key development has been the introduction of Higgs fields into the theory of weak interactions. These and other ideas of quantum field theory are described by Zeldovich in an article aimed at providing enlightenment for observational astrophysicists (Zeldovich, 1986). The Higgs field was introduced into the electro-weak theory of elementary particles in order to eliminate singularities in the theory and to endow the W^\pm and Z^0 bosons with masses. Precise measurement of the masses of these particles at CERN has confirmed the theory very precisely, although the Higgs particles themselves have not yet been found in accelerator experiments; the particle physics community confidently expects that these elusive particles will be discovered in the first experiments carried out at the Large Hadron Collider (LHC) at CERN in 2008. As described by Zeldovich, the Higgs fields have the property of being scalar fields, unlike the vector fields of electromagnetism or the tensor fields of General Relativity, and have negative pressure equations of state $p = -\varrho c^2$.

In the modern picture of the vacuum, there are zero-point fluctuations associated with the zero-point energies of all quantum fields. The stress-energy tensor of a vacuum has a negative pressure equation of state, $p = -\varrho c^2$. This pressure may be thought of as a ‘tension’ rather than a pressure. When such a vacuum expands, the work done $p dV$ in expanding from V to $V + dV$ is just $-\varrho c^2 dV$ so that, during the expansion, the mass-energy density of the negative pressure field remains constant. We can find the same result directly from (7.6). If the vacuum energy density is to remain constant, $\varrho_{\text{vac}} = \text{constant}$, it follows from that equation that $p = -\varrho c^2$.

Since vacuum fluctuations are now an integral part of modern physics, it is straightforward to work out what the cosmological vacuum energy should be. Carroll, Press and Turner have described how a theoretical value of Λ can be estimated using simple concepts from quantum field theory (Carroll et al., 1992). In their approach, they perform a standard analysis to estimate the energy density of the vacuum fields by integrating to a maximum wavenumber k_{\max} at which the theory breaks down. They find

$$\varrho_{\text{vac}} = \lim_{L \rightarrow \infty} \frac{E_0}{L^3} = \hbar \frac{k_{\max}^4}{16\pi^2} . \quad (7.33)$$

They take the energy at which conventional field theory breaks down due to quantum gravitational effects to occur at the Planck energy scale, $E^* \approx 10^{19} \text{ GeV}$ and hence, if $k_{\max} = E^*/\hbar$, $\varrho_{\text{vac}} \approx 10^{95} \text{ kg m}^{-3}$.

A similar argument is presented by Peacock in his splendid book *Cosmological Physics* (Peacock, 2000). Heisenberg’s Uncertainty Principle states that a virtual pair of particles of mass m can exist for a time $t \sim \hbar/mc^2$, corresponding to a maximum separation $x \sim \hbar/mc$. Hence, the typical density of the vacuum fields is $\varrho \sim m/x^3 \approx c^3 m^4/\hbar^3$. The mass density in the vacuum fields is unchanging with cosmic epoch and so, adopting the Planck mass for $m = m_{\text{Pl}} = (\hbar c/G)^{1/2} = 5.4 \times 10^{-8} \text{ kg} \equiv 3 \times 10^{19} \text{ GeV}$, the mass density corresponds to about $10^{97} \text{ kg m}^{-3}$.

There is now compelling evidence that Λ is finite with mass density corresponding to $\varrho_\Lambda \approx 6 \times 10^{-27} \text{ kg m}^{-3}$, about 10^{120} times less than the predicted value. This is quite a problem, but it should not be passed over lightly. If the inflationary picture of the very early Universe is taken seriously, this is exactly the type of field which drove the inflationary expansion. Then, we have to explain why ϱ_Λ decreased by a factor of about 10^{120} at the end of the inflationary era. In this context, 10^{-120} looks remarkably close to zero, which would correspond to the standard Friedman picture with $\Lambda = 0$, but this evidently cannot be the type of Universe we live in.

Thus, it is now quite natural to believe that there are indeed forces in nature which can provide Zeldovich’s ‘repulsion of the vacuum’ and to associate a certain mass density ϱ_Λ with the energy density of the vacuum, or the *dark energy*, at the present epoch. It is convenient to rewrite the formalism we have developed above in terms of a density parameter Ω_Λ associated with the dark energy as follows. We begin with (7.30) in the form:

$$\ddot{a} = -\frac{4\pi Ga}{3} \left(\varrho_m + \varrho_v + \frac{3p_v}{c^2} \right) , \quad (7.34)$$

where, in addition to the density of ‘dust’ ϱ_m , we have included the mass density ϱ_v and pressure p_v of the vacuum fields. Since $p_v = -\varrho_v c^2$, it follows that

$$\ddot{a} = -\frac{4\pi Ga}{3} (\varrho_m - 2\varrho_v) . \quad (7.35)$$

As the Universe expands, $\varrho_m = \varrho_0/a^3$ and $\varrho_v = \text{constant}$. Therefore,

$$\ddot{a} = -\frac{4\pi G\varrho_0}{3a^2} + \frac{8\pi G\varrho_v a}{3} . \quad (7.36)$$

Equations (7.32) and (7.36) have precisely the same dependence of the ‘cosmological term’ upon the scale factor a and so we can formally identify the cosmological constant with the vacuum mass density.

$$\Lambda = 8\pi G Q_v . \quad (7.37)$$

At the present epoch, $a = 1$ and so

$$\ddot{a}(t_0) = -\frac{4\pi G \varrho_0}{3} + \frac{8\pi G Q_v}{3} . \quad (7.38)$$

A density parameter associated with Q_v can now be introduced, in exactly the same way as the density parameter Ω_0 was defined:

$$\Omega_\Lambda = \frac{8\pi G Q_v}{3H_0^2} \quad \text{and so} \quad \Lambda = 3H_0^2 \Omega_\Lambda . \quad (7.39)$$

The dynamical equations (7.30) and (7.31) can now be written

$$\ddot{a} = -\frac{\varrho_0 H_0^2}{2a^2} + \Omega_\Lambda H_0^2 a ; \quad (7.40)$$

$$\dot{a}^2 = \frac{\varrho_0 H_0^2}{a} - \frac{c^2}{\mathfrak{N}^2} + \Omega_\Lambda H_0^2 a^2 . \quad (7.41)$$

We now substitute the values of a and \dot{a} at the present epoch, $a = 1$ and $\dot{a} = H_0$, into (7.41) to find the relation between the curvature of space, ϱ_0 and Ω_Λ :

$$\frac{c^2}{\mathfrak{N}^2} = H_0^2 [(\varrho_0 + \Omega_\Lambda) - 1] , \quad (7.42)$$

or

$$\kappa = \frac{1}{\mathfrak{N}^2} = \frac{[(\varrho_0 + \Omega_\Lambda) - 1]}{(c^2/H_0^2)} . \quad (7.43)$$

Thus, the condition that the spatial sections are flat Euclidean space becomes

$$(\varrho_0 + \Omega_\Lambda) = 1 . \quad (7.44)$$

We recall that the radius of curvature R_c of the spatial sections of these models change with scale factor as $R_c = a\mathfrak{N}$ and so, if the space curvature is zero now, it must have been zero at all times in the past.

7.3.2 Varying the Equation of State of the Vacuum Energy

A further generalisation of the formalism given above is to suppose that the equation of state has the generic form $p_i = w_i \varrho_i c^2$. We can then use the relativistic energy conservation equation (7.6) to find the variation of the density with scale factor a .

Equation (7.6) becomes

$$\frac{d\varrho_i}{da} + 3 \frac{\left(\varrho_i + \frac{p_i}{c^2} \right)}{a} = 0 ; \quad \frac{d\varrho_i}{da} = -\frac{3\varrho_i(1+w_i)}{a} . \quad (7.45)$$

Hence, integrating, the variation of the density with scale factor is

$$\varrho_i \propto a^{-3(1+w_i)} . \quad (7.46)$$

This result makes a lot of sense. In the case of cold matter, $w_i = 0$ and so $\varrho \propto a^{-3}$.

For photons and ultrarelativistic matter, $w_i = 1/3$ and so $\varrho \propto a^{-4}$. For standard dark energy, $w_i = -1$ and $\varrho = \text{constant}$. It is therefore straightforward to repeat the analysis of the previous section to find the relations between the density parameter in the species i and the geometrical properties of the world models. We leave it as an exercise for the reader to show that the results of these calculations are:

$$\dot{a} = -\frac{\varrho_0 H_0^2}{2a^2} - (1+3w_i) \frac{\Omega_{10} H_0^2}{2a^{2+3w_i}} , \quad (7.47)$$

where the density parameter at the present epoch of the species i , Ω_{10} , is given by

$$\Omega_{10} = \frac{8\pi G \varrho_{10}}{3H_0^2} . \quad (7.48)$$

The expression for \dot{a} becomes

$$\dot{a}^2 = \frac{\varrho_0 H_0^2}{a} + \frac{\Omega_{10} H_0^2}{a^{1+3w_i}} - \frac{c^2}{\mathfrak{N}^2} . \quad (7.49)$$

Inserting the values of $a = 1$ and $\dot{a} = H_0$ at the present epoch, we find

$$\frac{c^2}{\mathfrak{N}^2} = H_0^2 [(\varrho_0 + \Omega_{10}) - 1] , \quad (7.50)$$

and so

$$\kappa = \frac{1}{\mathfrak{N}^2} = \frac{[(\varrho_0 + \Omega_{10}) - 1]}{(c^2/H_0^2)} . \quad (7.51)$$

The reason for carrying out this extension of the standard formalism is that we can use these results to estimate w_i directly from the observations. Note also that (7.51) shows that the condition for flat spatial geometry is that all the contributions to Ω_0 and Ω_{10} sum to unity,

$$\Omega_0 + \sum_i \Omega_{10} = 1 . \quad (7.52)$$

7.3.3 The Dynamics of World Models with $\Lambda \neq 0$: General Considerations

The dynamics of world models with $\Lambda \neq 0$ are of special importance in the light of the most recent estimates of the values of cosmological parameters. First of all, we

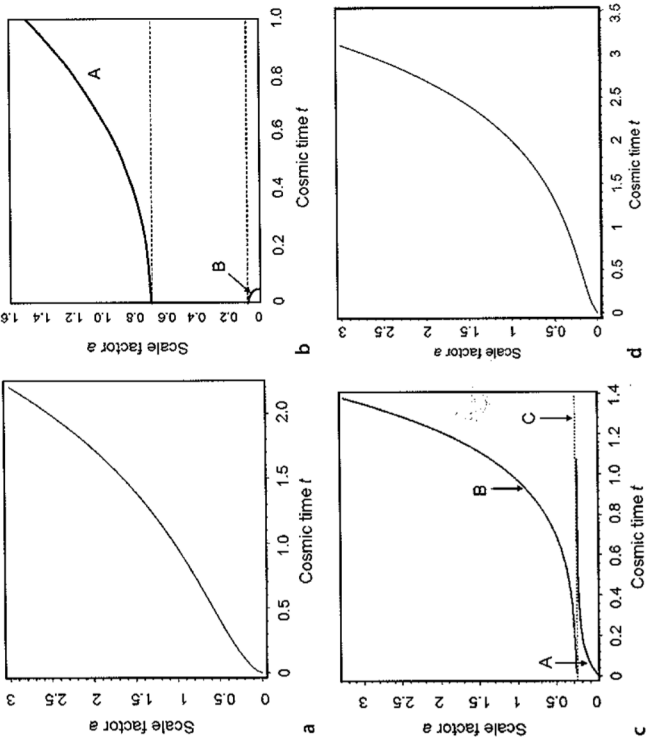


Fig. 7.3a-d. Examples of the dynamics of world models in which $\Lambda \neq 0$ (Bondi, 1960). Models **a** and **d** are referred to as Lemaitre models. In **a**, the model parameters are $\Omega_0 = 0.3$ and $\Omega_\Lambda = 0.7$, a favoured model according to current best estimates of these parameters. **b** This ‘bouncing’ model has $\Omega_0 = 0.05$ and $\Omega_\Lambda = 2$. The zero of cosmic time has been set to the value when $\dot{a} = 0$. The loci are symmetric in cosmic time with respect to this origin. **c** This model is an Eddington–Lemaitre model which is stationary at redshift $z_c = 3$, corresponding to scale factor $a = 0.25$. In **d**, the model parameters are $\Omega_0 = 0.01$ and $\Omega_\Lambda = 0.99$ and the age of the Universe can far exceed H_0^{-1}

behaviour corresponds to exponentially collapsing and expanding de Sitter solutions

$$\dot{a}^2 = H_0^2 [\Omega_\Lambda a^2 - (\Omega_\Lambda - 1)] , \quad (7.56)$$

which has solution

$$a = \left(\frac{\Omega_\Lambda - 1}{\Omega_\Lambda} \right)^{1/2} \cosh \Omega_\Lambda^{1/2} H_0 \tau , \quad (7.57)$$

where the time $\tau = t - t_{\min}$ is measured from the time at which the model ‘bounced’, that is, from the time at which $a = a_{\min}$. In all cases in which the models bounce, the variation of a with cosmic time is symmetrical about a_{\min} . Their asymptotic

discuss some general considerations of the dynamics of these models and then look in more detail at the range of models which are likely to be relevant for our future studies.

Models with $\Lambda < 0$ are not of a great deal of interest because the net effect is to incorporate an attractive force in addition to gravity which slows down the expansion of the Universe. The one difference from the models with $\Lambda = 0$ is that, no matter how small the values of Ω_Λ and Ω_0 are, the universal expansion is eventually reversed, as may be seen by inspection of (7.32).

Models with $\Lambda > 0$, $\Omega_\Lambda > 0$ are much more interesting because a positive cosmological constant leads to a repulsive force which opposes the attractive force of gravity. In each of these models, there is a minimum rate of expansion \dot{a}_{\min} which is found by setting $\ddot{a} = 0$ in (7.40). The corresponding value of the scale factor and minimum rate of expansion are

$$a_{\min} = (\Omega_0/2\Omega_\Lambda)^{1/3} , \quad (7.53)$$

$$\dot{a}_{\min}^2 = \frac{3H_0^2}{2} (2\Omega_\Lambda \Omega_0^2)^{1/3} - \frac{c^2}{\mathcal{R}^2} . \quad (7.54)$$

If the right-hand side of (7.54) is greater than zero, the dynamical behaviour shown in Fig. 7.3a is found. For large values of a , the dynamics become those of the de Sitter universe

$$a(t) \propto \exp \left[\left(\frac{\Lambda}{3} \right)^{1/2} t \right] = \exp \left(\Omega_\Lambda^{1/2} H_0 t \right) . \quad (7.55)$$

If the right-hand side of (7.54) is less than zero, there exists a range of scale factors for which no solution exists and it can be shown readily that the function $a(t)$ has two branches, as illustrated in Fig. 7.3b. For the branch B, the Universe never expanded to sufficiently large values of a that the repulsive effect of the Λ -term can prevent the Universe collapsing. In the case of branch A, the dynamics are dominated by the Λ -term; the repulsive force is so strong that the Universe never contracted to such a scale that the attractive force of gravity could overcome its influence. In the latter model, there was no initial singularity – the Universe ‘bounced’ under the influence of the Λ -term. In the limiting case in which the density of matter is zero, $\Omega_0 = 0$, the dynamics of the model are described by

$$a = \left(\frac{\Omega_\Lambda - 1}{\Omega_\Lambda} \right)^{1/2} \exp \left(\pm \Omega_\Lambda^{1/2} H_0 t \right) . \quad (7.58)$$

In these ‘bouncing’ Universes, the smallest value of a , a_{\min} , corresponds to the largest redshifts which objects could have.

The most interesting cases are those for which $\dot{a}_{\min} \approx 0$. The case where $\dot{a}_{\min} = 0$ is known as the *Eddington–Lemaitre model* and is illustrated in Fig. 7.3c. The literal interpretation of these models is either: A, the Universe expanded from an origin at some finite time in the past and will eventually attain a stationary state in the infinite

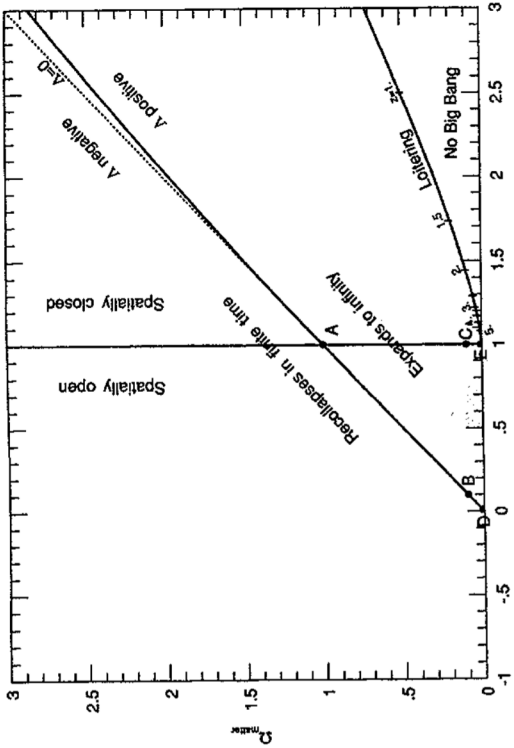


Fig. 7.4. The classification of the Friedman world models with $\Omega_0 \neq 0$ in a plot of Ω_0 against $\Omega_0 + \Omega_\Lambda$ (Carroll et al., 1992). The Eddington–Lemaître models lie along the line labelled ‘loitering’.

future; B, the Universe is expanding away from a stationary solution in the infinite past. The stationary state C is unstable because, if it is perturbed, the Universe moves either onto branch B, or onto the collapsing variant of branch A. In Einstein’s static Universe, the stationary phase occurs at the present day. From (7.53), the value of Λ corresponding to $\dot{a}_{\min} = 0$ is

$$\Lambda = \frac{3}{2}\Omega_0 H_0^2(1+z_c)^3 \quad \text{or} \quad \Omega_\Lambda = \frac{\Omega_0}{2}(1+z_c)^3, \quad (7.59)$$

where z_c is the redshift of the stationary state. The static Eddington–Lemaître models have $\dot{a} = 0$ for all time and so, setting the right-hand side of (7.41) equal to zero and substituting (7.59), we find a one-to-one relation between the mean density of matter in the Universe Ω_0 and the redshift of the stationary phase z_c ,

$$\Omega_0 = \frac{2}{(1+z_c)^3 - 3(1+z_c) + 2} = \frac{2}{z_c^2(z_c + 3)}. \quad (7.60)$$

This calculation is largely of academic interest nowadays. If a stationary, or near-stationary, state had occurred, the fact that galaxies and quasars are now observed with redshifts $z > 6$ suggests that $z_c > 6$ and so $\Omega_0 \leq 0.01$, which is at least an order of magnitude less than the total mass density in dark matter at the present epoch.

The properties of the world models with non-zero cosmological constant are conveniently summarised in a plot of Ω_0 against $\Omega_0 + \Omega_\Lambda$ presented by Carroll, Press and Turner (Fig. 7.4) (Carroll et al., 1992). The world models with $\Lambda = 0$ lie along the 45° line passing through zero on both axes. As shown by (7.43), the spatial geometry of the world model depends upon the value of $\Omega_0 + \Omega_\Lambda$, the value unity separating the open from closed geometries. The models which were stationary in the past, corresponding to the dividing line between those models which had a singular past and those which ‘bounced’, are given by (7.59) and (7.60), the values of the stationary redshifts being indicated along the locus to the bottom right of the diagram – Carroll, Press and Turner call these ‘loitering’ models. Finally, the diagram also shows the dividing line between those models which will eventually recollapse to a ‘big crunch’ in the future and those which will expand forever. This dividing line can also be found from (7.59) and (7.60) by requiring the models to tend to stationary phases in the future, for which the values of a are greater than one and the redshifts less than zero. For example, using (7.60), we find that the model which is stationary at a scale factor $a = 1.5$, corresponding to $(1+z_c) = 2/3$, has $\Omega_0 = 27/16 = 1.69$. The corresponding value of Ω_Λ from (7.59) is 0.25, so that $\Omega_0 + \Omega_\Lambda = 31/16 = 1.94$, which lies on the solid line separating the models which expand to infinity from those which collapse in a finite time in Fig. 7.4.

The models with positive cosmological constant can have ages greater than H_0^{-1} . In the limiting cases of Eddington–Lemaître models with $\dot{a}_{\min} = 0$ in the infinite past, for example, the Universe is infinitely old. A closely related set of models, with ages which can be greater than H_0^{-1} , are the Lemaître models which have values of

Ω_Λ such that the value of \dot{a}_{\min} is just greater than zero. An example of this type of model is shown in Fig. 7.3d.

As we will show in Chap. 15, there is now strong evidence that the spatial geometry of the Universe is flat, so that $\Omega_0 + \Omega_\Lambda$ is very close to unity. The dynamics of such spatially flat models with different combinations of Ω_0 and Ω_Λ are shown in Fig. 7.5. These models indicate how the age of the Universe can be greater than H_0^{-1} for large enough values of Ω_Λ .

7.4 Observations in Cosmology

Models with finite values of the cosmological constant dominate much of current cosmological thinking and so it is convenient to develop the expressions for the relations between observables and intrinsic properties in parallel for models with and without the Λ -term. The reason for including the results for world models with $\Omega_\Lambda = 0$ is that they can often be expressed analytically in closed form and so provide insight into the physics of the world models.

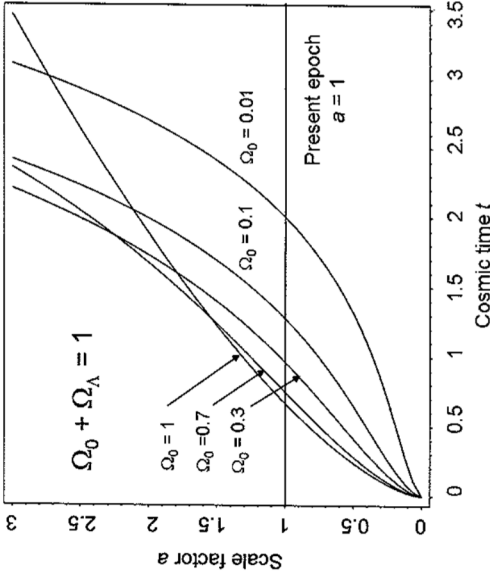


Fig. 7.5. The dynamics of spatially flat world models, $\Omega_0 + \Omega_\Lambda = 1$, with different combinations of Ω_0 and Ω_Λ . The abscissa is plotted in units of H_0^{-1} . The dynamics of these models can be compared with those shown in Fig. 7.2 which have $\Omega_\Lambda = 0$

7.4.1 The Deceleration Parameter

Just as Hubble's constant H_0 measures the expansion rate of the Universe at the present epoch, so we can define the present deceleration of the Universe $\ddot{a}(t_0)$. It is conventional to define the *deceleration parameter* q_0 to be the dimensionless deceleration at the present epoch through the expression

$$q_0 = -\left(\frac{\dot{a}\ddot{a}}{\dot{a}^2}\right)_{t_0}. \quad (7.61)$$

Substituting $a = 1$, $\dot{a} = H_0$ at the present epoch into the dynamical equation (7.40), we find

$$q_0 = \frac{\Omega_0}{2} - \Omega_\Lambda. \quad (7.62)$$

Equation (7.62) represents the present competition between the decelerating effect of the attractive force of gravity and the accelerating effect of the repulsive dark energy. Substituting the favoured values of $\Omega_0 = 0.3$ and $\Omega_\Lambda = 0.7$ (see Chaps. 8 and 15), we find $q_0 = -0.55$, showing that the Universe is accelerating at the present epoch because of the dominance of the dark energy.

7.4.2 The Cosmic Time–Redshift Relation

An important result for many aspects of astrophysical cosmology is the relation between cosmic time t and redshift z . Combining (7.41) and (7.42), we find

$$\dot{a} = H_0 \left[\Omega_0 \left(\frac{1}{a} - 1 \right) + \Omega_\Lambda (a^2 - 1) + 1 \right]^{1/2}. \quad (7.63)$$

Because $a = (1+z)^{-1}$,

$$\frac{dz}{dt} = -H_0(1+z)[(1+z)^2(\Omega_0 z + 1) - \Omega_\Lambda z(z+2)]^{1/2}. \quad (7.64)$$

The cosmic time t measured from the Big Bang follows immediately by integration from $z = \infty$ to z ,

$$t = \int_0^t dt = -\frac{1}{H_0} \int_{\infty}^z \frac{dz}{(1+z)[(1+z)^2(\Omega_0 z + 1) - \Omega_\Lambda z(z+2)]^{1/2}}. \quad (7.65)$$

Let us evaluate this integral separately for models with $\Omega_\Lambda = 0$ and for finite Ω_Λ . **Models with $\Omega_\Lambda = 0$.** For $\Omega_0 > 1$, we can write $x = (\Omega_0 - 1)a/\Omega_0 = (\Omega_0 - 1)/\Omega_0(1+z)$, and then the cosmic time–redshift relation becomes

$$t(z) = \frac{\Omega_0}{H_0(\Omega_0 - 1)^{3/2}} [\sin^{-1} x^{1/2} - x^{1/2}(1-x)^{1/2}]. \quad (7.66)$$

For $\Omega_0 < 1$, we write $y = (1-\Omega_0)a/\Omega_0 = (1-\Omega_0)/\Omega_0(1+z)$, and then the cosmic time–redshift relation becomes

$$t(z) = \frac{\Omega_0}{H_0(1-\Omega_0)^{3/2}} [y^{1/2}(1+y)^{1/2} + \sinh^{-1} y^{1/2}]. \quad (7.67)$$

For large redshifts, $z \gg 1$, $\Omega_0 z \gg 1$, (7.66) and (7.67) reduce to

$$t(z) = \frac{2}{3H_0\Omega_0^{1/2}} z^{-3/2}. \quad (7.68)$$

We can find the present age of the Universe for the different world models by integrating from $z = 0$ to $z = \infty$.

$$t_0 = \frac{\Omega_0}{H_0(\Omega_0 - 1)^{3/2}} \left[\sin^{-1} \left(\frac{\Omega_0 - 1}{\Omega_0} \right)^{1/2} - \frac{(\Omega_0 - 1)^{1/2}}{\Omega_0} \right] \quad \text{if } \Omega_0 > 1;$$

$$t_0 = \frac{2}{3H_0} \quad \text{if } \Omega_0 = 1;$$

$$t_0 = \frac{\Omega_0}{H_0(1-\Omega_0)^{3/2}} \left[\frac{(1-\Omega_0)^{1/2}}{\Omega_0} - \sinh^{-1} \left(\frac{1-\Omega_0}{\Omega_0} \right)^{1/2} \right] \quad \text{if } \Omega_0 < 1.$$

The age of the Universe is a monotonic function of Ω_0 . The useful simple cases are those for the critical model $\Omega_0 = 1$ for which the present age of the Universe is $(2/3)H_0^{-1}$ and the empty model, $\Omega_0 = 0$, for which it is H_0^{-1} . For $\Omega_0 = 2$, the age of the Universe is $0.571 H_0^{-1}$.

Models with $\Omega_\Lambda \neq 0$. The time-redshift relation for any of the models with finite Ω_Λ can be found by integration of (7.65). The models with zero curvature are of particular interest and there is a simple analytic solution for the cosmic time-redshift relation for these models. From (7.44), the condition that the curvature of space is zero, $\mathfrak{R} \rightarrow \infty$, is $\Omega_0 + \Omega_\Lambda = 1$. Then, from (7.65),

$$t = \int_0^r dt = -\frac{1}{H_0} \int_{\infty}^z \frac{dz}{(1+z)[\Omega_0(1+z)^3 + \Omega_\Lambda]^{1/2}}. \quad (7.69)$$

The cosmic time-redshift relation becomes

$$t = \frac{2}{3H_0\Omega_\Lambda^{1/2}} \ln \left(\frac{1+\cos\theta}{\sin\theta} \right) \quad \text{where} \quad \tan\theta = \left(\frac{\Omega_0}{\Omega_\Lambda} \right)^{1/2} (1+z)^{3/2}. \quad (7.70)$$

The present age of the Universe follows by setting $z = 0$

$$t_0 = \frac{2}{3H_0\Omega_\Lambda^{1/2}} \ln \left[\frac{1+\Omega_\Lambda^{1/2}}{(1-\Omega_\Lambda)^{1/2}} \right]. \quad (7.71)$$

This relation illustrates how it is possible to find a Friedman model which has age greater than H_0^{-1} and yet has flat spatial sections. For example, if $\Omega_\Lambda = 0.9$ and $\Omega_0 = 0.1$, the age of the world model would be $1.28H_0^{-1}$. For the popular world model with $\Omega_0 = 0.3$ and $\Omega_\Lambda = 0.7$, the age of the Universe is $0.964H_0^{-1}$, remarkably close to H_0^{-1} .

7.4.3 Distance Measures as a Function of Redshift

We can now complete our programme of finding expressions for the comoving radial distance coordinate r and the distance measure D . We recall that the increment of comoving radial coordinate distance is

$$dr = -\frac{c dt}{a(t)} = -c dt(1+z). \quad (7.72)$$

From (7.64),

$$\frac{dr}{a} = -\frac{c dt}{a} = \frac{c}{H_0} \frac{d z}{[(1+z)^2(\Omega_0 z + 1) - \Omega_\Lambda z(z+2)]^{1/2}}, \quad (7.73)$$

and so, integrating from redshift 0 to z , we find the expression for r ,

$$r = \frac{c}{H_0} \int_0^z \frac{dz}{[(1+z)^2(\Omega_0 z + 1) - \Omega_\Lambda z(z+2)]^{1/2}}. \quad (7.74)$$

Then, we can find the distance measure D by evaluating $D = \mathfrak{R} \sin(r/\mathfrak{R})$, where \mathfrak{R} is given by (7.42). Let us discuss first the case $\Omega_\Lambda = 0$.

Models with $\Omega_\Lambda = 0$. Integrating (7.74) with $\Omega_\Lambda = 0$ and $\Omega_0 > 1$, we find

$$\begin{aligned} r &= \frac{c}{H_0} \int_0^z \frac{dz}{(1+z)(\Omega_0 z + 1)^{1/2}} \\ &= \frac{2c}{H_0(\Omega_0 - 1)^{1/2}} \left[\tan^{-1} \left(\frac{\Omega_0 z + 1}{\Omega_0 - 1} \right)^{1/2} - \tan^{-1} (\Omega_0 - 1)^{-1/2} \right]. \end{aligned} \quad (7.75)$$

If $\Omega_0 < 1$, the inverse tangents are replaced by inverse hyperbolic tangents. After some further straightforward algebra, we find that

$$D = \frac{2c}{H_0\Omega_0^2(1+z)} \{ \Omega_0 z + (\Omega_0 - 2)[(\Omega_0 z + 1)^{1/2} - 1] \}. \quad (7.77)$$

This is the famous formula first derived by Mattig (Mattig, 1959). Although the integral has been found for the case of spherical geometry, it turns out that the formula is correct for all values of Ω_0 . In the limit of the empty, or Milne, world model, $\Omega_0 = 0$, (7.77) becomes

$$D = \frac{cz}{H_0} \frac{\left(1 + \frac{z}{2}\right)}{(1+z)}. \quad (7.78)$$

The variations of r and D with redshift for a range of standard world models are shown in Figs. 7.6a and 7.7.

Models with $\Omega_\Lambda \neq 0$. Solutions of the integral (7.74) for the case $\Omega_\Lambda \neq 0$ may be found in terms of elliptic functions but we do not wish to enter into that exercise here. It is generally easier to evaluate the comoving radial distance coordinate r and distance measure $D = \mathfrak{R} \sin(r/\mathfrak{R})$ by numerical integration. Some examples of these computations for flat world models with $\Omega_0 + \Omega_\Lambda = 1$ for different values of Ω_0 are shown in Fig. 7.6b. Notice that, because the geometry of these world models is flat $\mathfrak{R} = \infty$, $r = D$.

Figures 7.6 and 7.7 repay some study. For the models with $\Omega_\Lambda = 0$, the smaller the value of Ω_0 , the greater the comoving radial distance coordinate at a given redshift. We can interpret this result in terms of the light travel time along the radial geodesic from the source to the observer on Earth. The smaller the deceleration of the expansion, the greater the distance light has to travel to reach the Earth. Likewise, for the models with finite values of Ω_Λ , the greater the value of Ω_Λ , the greater the stretching of the cosmic time-scale and so the greater the light travel time to the Earth. The comparison of Figs. 7.6a and 7.7 shows the influence of the curved spatial geometry upon the observed properties of distant objects. For the case $\Omega_0 = 1$, D and r are the same in the two diagrams since the geometry is flat. For other values of Ω_0 , the loci of the distance measure D in Fig. 7.7 diverge with respect to this model because of their hyperbolic ($\Omega_0 < 1$) and spherical ($\Omega_0 > 1$) geometries.

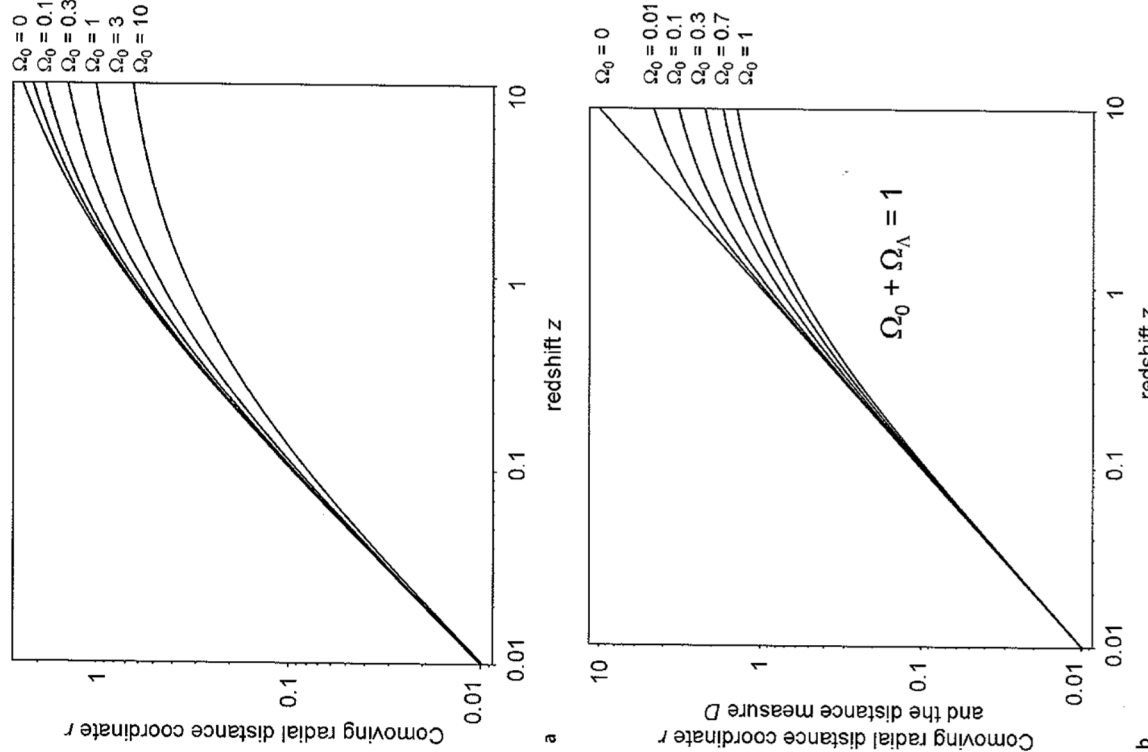


Fig. 7.6a,b. The variation with redshift of **a** the radial comoving distance coordinate r for models with $\Omega_A = 0$, and **b** the comoving radial distance coordinate r for models with $\Omega_A \neq 0$. Because the geometry is flat, $\Omega_0 + \Omega_A = 1$, $r = (c/H_0)z$. In both diagrams, r and D are measured in units of c/H_0

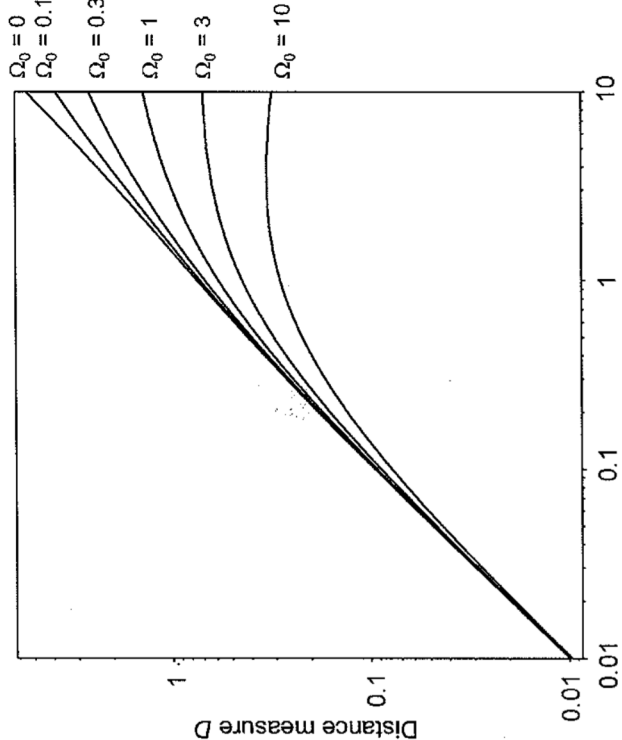


Fig. 7.7. The variation with redshift of the distance measure D for Friedman world models with $\Omega_A = 0$. D is measured in units of c/H_0

7.4.4 Angular Diameter–Redshift Relations

Models with $\Omega_A = 0$. In Fig. 7.8a, the variation of the observed angular size of a rigid rod of unit proper length is shown using the expressions (5.54) and (7.77) – this type of angular diameter is known as a *metric angular diameter*. Except for the empty world model, $\Omega_0 = 0$, there is a minimum in the angular diameter–redshift relation which occurs at $z = 1.25$ for the critical model, $\Omega_0 = 1$, and at $z = 1$ if $\Omega_0 = 2$. The reason for the minimum in the angular diameter–redshift relation is a combination of two effects. The first is the curved spatial geometry of the world models and the second, and more important, is the fact that a rigid rod occupies

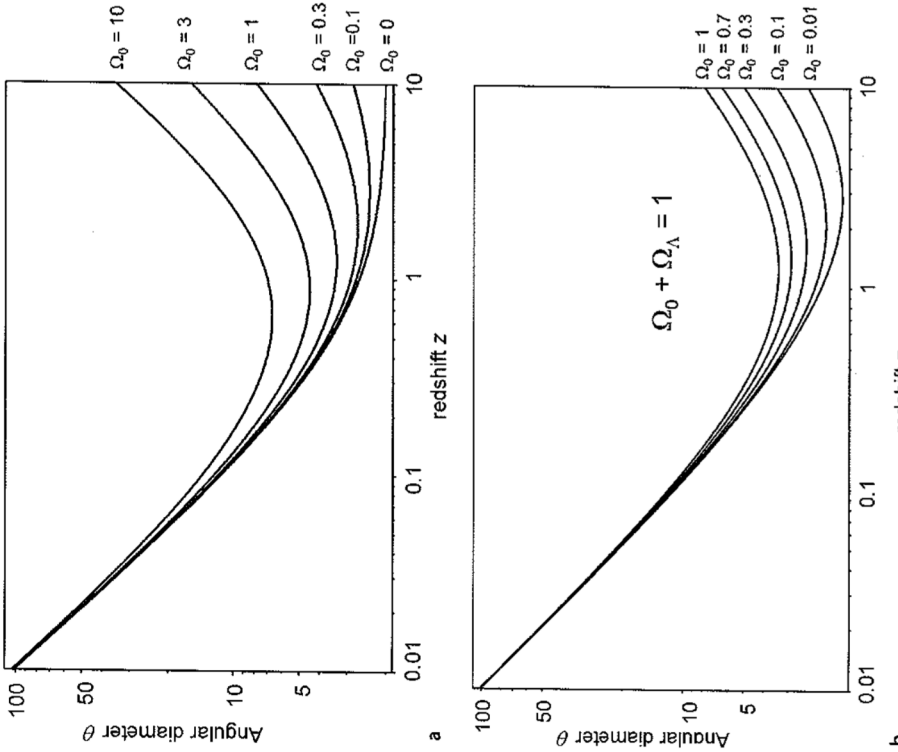


Fig. 7.8. **a** The variation of the angular diameter of a rigid rod of unit proper length with redshift for world models with $\Omega_\Lambda = 0$. **b** The variation of the angular diameter of a rigid rod of unit proper length with redshift for world models with finite values of Ω_Λ and flat spatial geometry, $\Omega_0 + \Omega_\Lambda = 1$. In both diagrams, c/H_0 has been set equal to unity

a larger fraction of the celestial sphere at a large redshift, by the factor $(1+z)$ which appears in (5.54).

Metric angular diameters are different from the types of angular diameter which are often used to measure the sizes of galaxies. The latter are often defined to some limiting surface brightness and so, since bolometric surface brightnesses vary with

redshift as $(1+z)^{-4}$, angular sizes measured to the same limiting surface brightness at a wide range of redshifts are not rigid rods of fixed proper length. The angular diameter–redshift relation can be worked out for *isophotal angular diameters*, but this requires knowledge of the K-corrections to be applied as a function of radius within the galaxy.

Models with $\Omega_\Lambda \neq 0$. The corresponding metric angular diameter–redshift relations for models with flat spatial geometry and finite values of Ω_Λ are shown in Fig. 7.8b. All these models have minima at some redshift, reflecting the fact that $r(z)$ ‘saturates’ at large redshifts (Fig. 7.6b) and the $(1+z)$ term in the expression (5.54) dominates the dependence upon redshift.

7.4.5 Flux Density–Redshift Relations

Models with $\Omega_\Lambda = 0$ and $\Omega_A \neq 0$. The observed flux density of a source of unit luminosity per unit frequency interval at frequency ν_0 with a power law spectrum $L(\nu) \propto \nu^{-1}$ is given by (5.65) with the distance measure D given by (7.77) for models with $\Omega_\Lambda = 0$ (Fig. 7.9a). The corresponding diagram for flat spatial models with $\Omega_\Lambda \neq 0$ are shown in Fig. 7.9b. Comparison of (5.65) and (5.66) shows that, because we have taken the spectral index to be $\alpha = 1$, these are also the variations of the bolometric flux density with redshift, in both cases. For galaxies, the detailed form of the spectrum has to be taken into account and this is often done using the K-corrections described by (5.69), (5.70) and (5.71). Figure 7.9 illustrates the very considerable challenge involved in attempting to distinguish between world models using the redshift–apparent magnitude, or flux density–redshift, relation. Objects with remarkably standard luminosities need to be used to have a hope of making progress. Fortunately, this has been achieved with the use of the Type Ia supernovae.

Ghost images. A unique feature of the Lemaitre world models is the possible appearance of *ghost images*. In the Eddington–Lemaitre models, the curvature of space κ is positive, as may be seen from the location of the ‘boiting’ line in Fig. 7.4. Those models which have d_{\min} just greater than zero also have closed spherical spatial sections, as may also be seen in Fig. 7.4. Since the expansion almost stops at redshift z_c , there is time for electromagnetic waves to propagate from the source to the observer a number of times around the closed geometry of the Universe. In principle, the same object may be observed in diametrically opposite directions, or multiply in the same position on the sky, although at different redshifts and consequently at different times in its life-history.

To illustrate this behaviour, consider the case of the Eddington–Lemaitre model which is stationary at redshift $z_c = 3$. In this case, the density parameter can be found from (7.60), $\Omega_0 = 1/27$, and the value of Ω_Λ from (7.59), $\Omega_\Lambda = 32/27$. Consequently, the radius of curvature of the closed geometry is $R = (27/6)^{1/2}(c/H_0)$. Inserting these values into (7.74) and integrating, we find the relation between r/\mathfrak{R} and redshift shown in Fig. 7.10. The values of $r/\mathfrak{R} = \pi, 2\pi, 3\pi$ and 4π are shown. It can be seen that r/\mathfrak{R} tends to infinity as the redshift approaches the stationary value $z_c = 3$.

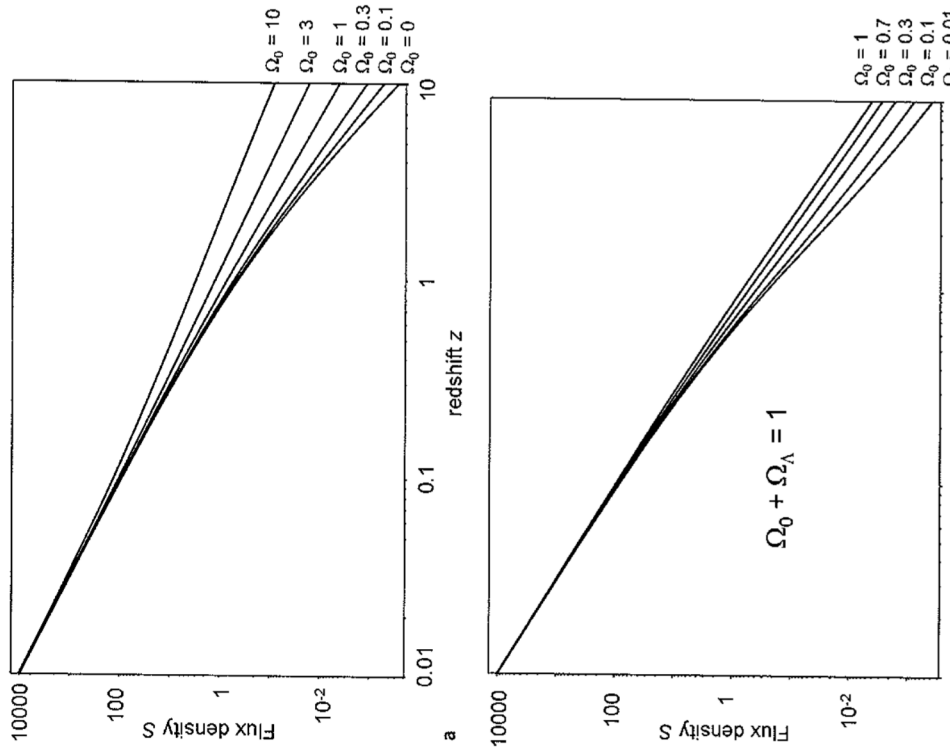


Fig. 7.9. The variation of the flux density of a source of luminosity 1 W Hz^{-1} with a power law spectrum $L(v) \propto v^{-1}$ with redshift. In both diagrams, $c/H_0 = 1$. Comparison of (5.65) and (5.66) shows that, since the spectral index $\alpha = 1$, these relations are the same as the variations of bolometric flux densities with redshift. **a** World models with $\Omega_0 + \Omega_\Lambda = 0$. **b** World models with finite values of Ω_Λ and flat spatial geometry $\Omega_0 + \Omega_\Lambda = 1$

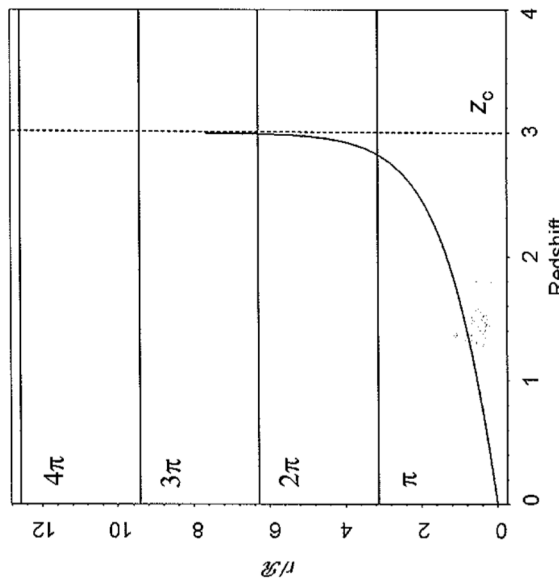


Fig. 7.10. The function r/R as a function of redshift z for the Eddington-Lemaître model which is stationary at redshift $z_c = 3$

The flux density-redshift relation for a source with spectral index $\alpha = 1$, defined by $S \propto v^{-\alpha}$, is

$$S \propto \frac{1}{[r \sin(r/R)]^2 (1+z)^2}. \quad (7.79)$$

It can therefore be seen that there is a first minimum in the flux density-redshift relation corresponding to $r/R = \pi/2$ and the observed flux density diverges at $r/R = \pi$, corresponding to redshift $z = 2.825$. This behaviour is repeated in the intervals $\pi < r/R < 2\pi, 2\pi < r/R < 3\pi, 3\pi < r/R < 4\pi, \dots$, the corresponding redshifts being $2.9923, 2.99967, 2.999986$ and so on. The interpretation of these phenomena is that, at $r/R = \pi$, we observe the antipodal point in the spherical closed geometry to our own location in the Universe. We may think of the light from a galaxy at the antipodal point being focussed on our own Galaxy at $z = 0$. In the case $r/R = 2\pi$, we observe our own locality, but as it was at the redshift $z = 2.9923$. These repeated images occur indefinitely as $z \rightarrow z_c$.

A corollary of this behaviour is that we can observe the same object in opposite directions in the sky, provided it has a very long lifetime. The radiation sets off in opposite directions from the source in the closed spherical geometry. If the source is observed at the redshift corresponding to r/R , there will be an image of the source at an earlier time in the opposite direction with redshift corresponding to $2\pi - r/R$.

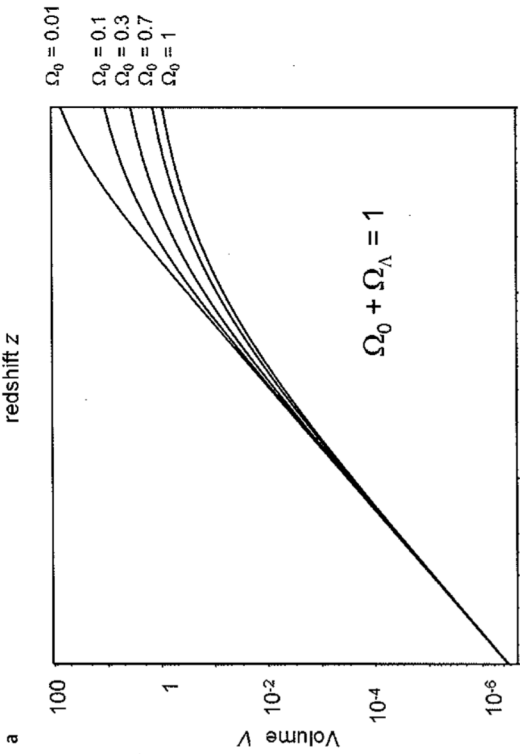


Fig. 7.11. **a** The variation of the comoving volume within redshift z for world models with $\Omega_A = 0$. **b** The variation of the comoving volume within redshift z for flat world models with finite values of Ω_Λ

Similar results are found in Lemaître models which do not quite reach the stationary state but have slightly positive values of \dot{a}_{\min} . They would lie just slightly above the ‘loitering’ line in Fig. 7.4. These models have to be rather finely tuned for the effect to be observable.

The possibility of observing ‘ghost’ images does not occur in the Friedman models with $\Omega_A = 0$. It is left as an exercise for the reader to use (7.6) to show that in all closed Friedman models with $\Omega_A = 0$, r/\Re tends to $\pi/2$ as z tends to infinity. Since $r/\Re = \pi/2$ corresponds to light rays propagating from the minimum flux density in the closed geometry to the Earth, the possibility of observing the same source in opposite directions in the sky, or multiple images of the same object in the same direction, does not occur.

The reason for discussing this aspect of the Lemaître models is that, if such repeated ‘ghost’ images were found, this would be evidence that the Universe passed through a long quasi-stationary phase. Searches for such ghost images have been carried out using large catalogues of extragalactic radio sources, but no positive result has been reported.

7.4.6 The Comoving Volume Within Redshift z

This relation can be determined from (5.72) by integration using the familiar expressions for the element of comoving radial distance coordinate dr and the distance measure D .

Models with $\Omega_A = 0$. In these cases, there are convenient expressions for the three cases with $\kappa > 1$, $\kappa = 1$ and $\kappa < 1$. The expression (5.72) can be integrated for the case $\Omega_0 > 1$, $\Re = (c/H_0)(\Omega_0 - 1)^{-1/2}$ to give

$$V(z) = 2\pi\Re^3 \left(\frac{r}{\Re} - \frac{1}{2} \sin \frac{2r}{\Re} \right) = 2\pi\Re^3 \left(\sin^{-1} \frac{D}{\Re} - \frac{D}{\Re} \sqrt{1 - \frac{D^2}{\Re^2}} \right). \quad (7.80)$$

For the case $\Omega_0 < 1$, $\Re = (c/H_0)(1 - \Omega_0)^{-1/2}$,

$$V(z) = 2\pi\Re^3 \left(\frac{1}{2} \sinh \frac{2r}{\Re} - \frac{r}{\Re} \right) = 2\pi\Re^3 \left(\frac{D}{\Re} \sqrt{1 + \frac{D^2}{\Re^2}} - \sinh^{-1} \frac{D}{\Re} \right). \quad (7.81)$$

For the critical world model, $\Omega_0 = 1$, $\Re = \infty$, $r = D$ and so

$$V(z) = \frac{4\pi}{3} r^3. \quad (7.82)$$

Examples of the comoving volume within redshift z are shown in Fig. 7.11a. Notice in Fig. 7.11a the convergence of the enclosed volume at redshifts $z > 1$. One of the problems of finding large redshift objects can be appreciated from this diagram. Whereas, at small redshifts, the volume elements increase with redshift as $z^2 dz$, at large redshifts, $\Omega_0 z > 1$, $z > 1$, the volume elements decrease with increasing redshift as $z^{-3/2} dz$ and so per unit redshift interval there are fewer sources and they become rarer and rarer with increasing redshift, even if the comoving number density is constant.

Models with $\Omega_A \neq 0$. There is little alternative in general to numerical integration using the familiar expressions for the element of comoving radial distance coordinate dr and the distance measure D . The case of flat geometry, with $\Omega_0 + \Omega_A = 1$, is simpler since $D = r$. Some examples of the results for models with finite values of Ω_A are shown in Fig. 7.11b. The model with $\Omega_0 = 1$ appears on both Fig. 11a and b. It can be seen that there is greater enclosed volume in the models with finite Ω_A because of the stretching of the cosmological time-scale.

7.5 Angular Diameter Distances Between Any Two Redshifts

There are occasions when it is necessary to relate metric diameters as observed from locations other than the origin at $z = 0$. A good example is the geometry of gravitational lensing in which we need the angular diameter distance $D_A(z_i, z_j)$, meaning the angular diameter distance necessary to work out the physical size of an object which subtends an angle θ between redshifts z_i and z_j (see Sect. 4.6 and (4.40)). It is a useful exercise to derive the pleasant result presented by Blandford and Narayan for the appropriate angular diameter distance to be used for models with $\Omega_A = 0$ (Blandford and Narayan, 1992). The extension to models with $\Omega_A \neq 0$ follows the same line of development, but it is simplest to carry out these calculations by numerical integration.

Models with $\Omega_A = 0$. We begin with the expression for the comoving radial distance coordinate r_{ij} between redshifts z_i and z_j . By extension of (7.76), we find

$$\begin{aligned} r_{ij} &= \frac{2c}{H_0(\Omega_0 - 1)^{1/2}} \left[\tan^{-1} \left(\frac{\Omega_0 z_j + 1}{\Omega_0 - 1} \right)^{1/2} - \tan^{-1} \left(\frac{\Omega_0 z_i + 1}{\Omega_0 - 1} \right)^{1/2} \right] \\ &= \frac{2c}{H_0(\Omega_0 - 1)^{1/2}} \left[\tan^{-1} \frac{G_j}{(\Omega_0 - 1)^{1/2}} - \tan^{-1} \frac{G_i}{(\Omega_0 - 1)^{1/2}} \right], \end{aligned} \quad (7.83)$$

where $G_j = (\Omega_0 z_j + 1)^{1/2}$ and $G_i = (\Omega_0 z_i + 1)^{1/2}$. Using the summation formulae for inverse tangents, this can be rewritten

$$r_{ij} = \frac{2c}{H_0(\Omega_0 - 1)^{1/2}} \frac{\tan^{-1} N_1(\Omega_0 - 1)^{1/2}}{N_2}, \quad (7.84)$$

where $N_1 = (G_j - G_i)$ and $N_2 = (\Omega_0 - 1 + G_i G_j)$.

We now form the expression $\Re' \sin(r'_{ij}/\Re')$ in order to find the distance measure D_{ij} between the redshifts z_i and z_j . We need to use the radius of curvature of the spatial geometry \Re' and the comoving radial distance coordinate r'_{ij} at the redshift z_i , but these both scale as $a(t)$ and so, since $\Re = (c/H_0)/(\Omega_0 - 1)^{1/2}$,

$$\begin{aligned} \sin \frac{r'_{ij}}{\Re'} &= \sin \frac{r_{ij}}{\Re} = \sin \left[2 \tan^{-1} \frac{N_1(\Omega_0 - 1)^{1/2}}{N_2} \right] \\ &= \frac{2N_1 N_2 (\Omega_0 - 1)^{1/2}}{N_1^2 (\Omega_0 - 1) + N_2^2}. \end{aligned} \quad (7.85)$$

$$\begin{aligned} \frac{D_A(z_i, z_j)}{D_A(z_j, z_i)} &= \frac{(1+z_i)}{(1+z_j)}. \end{aligned} \quad (7.94)$$

This is precisely the *reciprocity theorem* which we alluded to in Sect. 5.5.4. The angular diameter distances to be used in opposite directions along the light cone differ by the ratio of the scale factors corresponding to the redshifts z_1 and z_2 . If we set $z_i = 0$ and $z_j = z$, we find

$$\begin{aligned} \frac{D_A(0 \rightarrow z)}{D_A(z \rightarrow 0)} &= \frac{1}{(1+z)}, \\ \text{as we demonstrated in Sect. 5.5.4.} \end{aligned} \quad (7.95)$$

Models with $\Omega_A \neq 0$. In place of (7.84), we write

$$r_{ij} = \frac{c}{H_0} \int_{z_i}^{z_j} \frac{dz}{[(1+z)^2(\Omega_0 z + 1) - \Omega_A z(z+2)]^{1/2}} \quad (7.96)$$

and then form $D_{ij} = \mathfrak{N} \sin(r_{ij}/\mathfrak{N})$ using the expression $\mathfrak{N}^2 = (c/H_0)^2 / [(\Omega_0 + \Omega_A) - 1]$. In the case of the flat models, $\mathfrak{N} \rightarrow \infty$ and so $D_{ij} = r_{ij}$ which simplifies the further analysis. These values of D_{ij} can be used directly in (7.90) and (7.91). This is an important set of computations since the D_{ij} are needed in order to work out the statistics of gravitationally lensed images expected in deep images of the sky.

7.6 The Flatness Problem

Hubble's constant was introduced in Section 5.5.2 where it was emphasised that, in general, it changes with cosmic epoch. We can find the variation of Hubble's constant with redshift from (7.63) by setting $a = (1+z)^{-1}$. Then,

$$H(z) = \frac{\dot{a}}{a} = H_0 [(1+z)^2(\Omega_0 z + 1) - \Omega_A z(z+2)]^{1/2}. \quad (7.97)$$

In the same way, we can define a density parameter Ω at any epoch through the definition $\Omega = 8\pi G\rho/3H^2$. For the case of 'dust' $\rho = \rho_0(1+z)^3$ and so

$$\begin{aligned} \Omega &= \frac{8\pi G}{3H^2} \rho_0 (1+z)^3 \\ &= \left[\frac{\Omega_0 z + 1}{1+z} \right] - \Omega_A \left[\frac{1}{(1+z)} - \frac{1}{(1+z)^3} \right]. \end{aligned} \quad (7.98) \quad (7.99)$$

Therefore at large redshifts $z \gg 1$, $\Omega_0 z \gg 1$, it can be seen that the terms in the second square bracket in the denominator of (7.99) tend to zero and the terms in the first square bracket tends to Ω_0 . Therefore, at large redshifts, $\Omega \rightarrow 1$, *whatever the value of Ω_0 at the present epoch*.

It is not surprising that the dark energy is unimportant dynamically at large redshifts because of the very different dependences of the matter and the dark energy densities upon redshift. Let us therefore set the term in Ω_A equal to zero and rewrite (7.99) as follows:

$$\left(1 - \frac{1}{\Omega}\right) = (1+z)^{-1} \left(1 - \frac{1}{\Omega_0}\right). \quad (7.100)$$

There are two ways of looking at this result. On the one hand, it reaffirms our conclusion from (7.29) that the dynamics of all the world models tend to those of the critical model in their early stages. On the other hand, it is remarkable that the Universe is as close as it is to the value $\Omega_0 = 1$ at the present day. If the value

of Ω_0 were significantly different from 1 in the distant past, then it would be very different from 1 now as can be seen from (7.100). There is nothing in the standard models which requires Ω_0 to take any particular value – it is simply a parameter which should be fixed as part of the initial conditions of our Universe.

As will be shown in Chaps. 8 and 15, the observational evidence strongly suggests that $\Omega_0 \approx 0.3$, which on its own means that the curvature of space κ must be close to zero at the present epoch. Indeed, as we will show in Chap. 15, the curvature of space as determined by the WMAP mission is quite remarkably close to zero. This is the origin of what is often referred to as the *flatness problem*, namely, that our Universe must have been very finely tuned indeed to the value $\Omega = 1$ in the distant past if it is to end up close to $\Omega_0 = 1$ now. This observation turns out to be one of the key pieces of empirical evidence for the *inflationary picture* of the early Universe.

7.7 Inhomogeneous World Models

The results derived above are exact for isotropic, homogeneous world models. The evidence discussed in Chap. 2 shows that the Universe is isotropic and homogeneous on the large scale but, on small scales, the Universe is very far from homogeneous. Matter is concentrated into stars and galaxies which are very large perturbations in the mean density. These perturbations cause deviations of the paths of light rays and it is important to understand their effect upon the results quoted above. We consider first the limiting case in which the matter distribution is so inhomogeneous that there is no matter within the light cone subtended by a distant object at the observer.

This problem was treated elegantly by Zeldovich using simple physical arguments (Zeldovich, 1964). Identical results are obtained more arduously from a general Riemannian approach to the propagation of light signals in inhomogeneous cosmological models. We consider the case of the critical Einstein–de Sitter world model, $\Omega_0 = 1$, $\Omega_A = 0$, for which the spatial geometry is flat, $\kappa = 0$, $\mathfrak{N} = \infty$.

If the Universe were so inhomogeneous that all the matter was condensed into point-like objects, there is only a small probability that there will be any matter within the light cone subtended by a distant object of small angular size. Because of the long-range nature of gravitational forces, however, the background metric remains the standard flat Einstein–de Sitter metric and the overall dynamics of the Universe are unaltered. The Robertson–Walker metric for the critical model can be written

$$\begin{aligned} ds^2 &= dt^2 - \frac{a^2(t)}{c^2} [dr^2 + r^2(d\theta^2 + \sin^2\theta d\phi^2)] \\ &= dt^2 - \frac{a^2(t)}{c^2} [dx^2 + dy^2 + dz^2], \end{aligned} \quad (7.101) \quad (7.102)$$

where $a(t) = (t/t_0)^{2/3}$ and $t_0 = \frac{2}{3}H_0$ is the present age of the Universe. The terms x , y and z are comoving coordinates referred to the present epoch t_0 .

First, we consider the homogeneous case. Consider the events A and B which correspond to the emission of light signals at cosmic time t from either end of

a standard rod of length L oriented at right angles to the line of sight at comoving radial distance coordinate r (Fig. 7.12a). Then, the interval between events is minus the square of a proper length

$$c^2 ds^2 = -a^2(t) r^2 d\theta^2 = -a^2(t) dy^2 = -L^2. \quad (7.103)$$

Since $a(t) = (1+z)^{-1}$, we recover the result of Sects. 5.5.3 and 7.4.4,

$$d\theta = \frac{L(1+z)}{r}, \quad (7.104)$$

where $r = D = (2c/H_0)[1 - (1+z)^{-1/2}]$ for the Einstein-de Sitter model. Notice that, in the homogeneous case, the angle between the light rays $d\theta$ remains a constant during propagation from the source to the observer. This fundamental result is true for all isotropic world models and is a consequence of the postulates of isotropy and homogeneity.

In the model of an inhomogeneous Universe, we consider the propagation of the light rays in this background metric, but include in addition the effect of the absence of matter within the light cone subtended by the source at the observer. As discussed in Sect. 4.6, the angular deflection of a light ray by a point mass, or by an axially symmetric distribution of mass at the same distance, is

$$\frac{4GM(< p)}{pc^2}, \quad (7.105)$$

where $M(< p)$ is the mass within ‘collision parameter’ p , that is, the distance of closest approach of the light ray to the point mass (Fig. 4.18b). Figure 7.12b shows an idealised model for the propagation of the rays along the light cone, assuming the light paths are known. Because of the principle of superposition,

Density boundary

Figure 7.12a illustrates the deflection of light rays by a disc of material within the light cone subtended by the distant object AB. Figure 7.12b illustrates the divergence of a light ray because of the ‘negative’ mass, indicated by the grey shaded area, due to the absence of a disc of material in the interval dl within the light cone (Zeldovich, 1964).

$$\begin{aligned} \Delta\theta &= \frac{4G dM(< p)}{pc^2}. & (7.106) \\ \frac{d\theta}{dl} &= \frac{4\pi G p q(t)}{c^2}. & (7.107) \end{aligned}$$

We now convert to comoving coordinates $\theta = dy/dx$, $l = a(t)x$, $p = a(t)y$. For the Einstein-de Sitter model, $q(t) = q_0(1+z)^3$ with $q_0 = 3H_0^2/8\pi G$ and

$$x = \frac{2c}{H_0} [1 - (1+z)^{-1/2}]. \quad (7.108)$$

If we write $2c/H_0 = x_0$, then $(1+z) = x_0^2/(x_0 - x)^2$ and hence

$$\frac{d^2y}{dx^2} = \frac{6y}{(x_0 - x)^2}. \quad (7.109)$$

This equation can be solved using a series trial function $y = \sum_n a_n(x_0 - x)^n$, for which the solution can be written

$$y = a_3(x_0 - x)^3 + a_{-2}(x_0 - x)^{-2}. \quad (7.110)$$

Fitting the boundary conditions, namely that, at $x = y = 0$, the angle subtended by the source is $\Theta = dy/dx$, we find

$$y = \frac{2c\Theta}{5H_0}(1+z)[1 - (1+z)^{-5/2}]. \quad (7.111)$$

Therefore, since $L = a(t)y = y/(1+z)$, the final result is

$$L = \frac{2c\Theta}{5H_0}[1 - (1+z)^{-5/2}]. \quad (7.112)$$

Corresponding results have been obtained for Friedman models with $\Omega_0 \neq 1$ by Dashhevsky and Zeldovich and by Dyer and Roeder (Dashhevsky and Zeldovich, 1964).

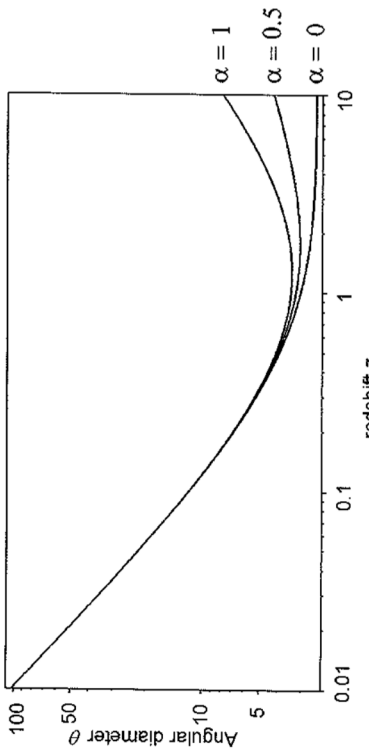


Fig. 7.13. Comparison between the angular diameter–redshift relation in the homogeneous, uniform Einstein–de Sitter world model ($\alpha = 1$), the same background model in which there is no mass within the light cone subtended by the source ($\alpha = 0$) and the case in which half of the total mass is uniformly distributed and the rest is contained in point masses ($\alpha = 0.5$)

1964; Dyer and Roeder, 1972). In these cases, if $\Omega_0 > 1$,

$$\begin{aligned} L &= \frac{3c\Omega_0^2\Theta}{4H_0(\Omega_0 - 1)^{5/2}} \left[\sin^{-1}\left(\frac{\Omega_0 - 1}{\Omega_0}\right)^{1/2} - \sin^{-1}\left(\frac{\Omega_0 - 1}{\Omega_0(1+z)}\right)^{1/2} \right] \\ &\quad - \frac{3c\Omega_0\Theta}{4H_0(\Omega_0 - 1)^2} \left[1 - \frac{(1 + \Omega_0 z)^{1/2}}{(1+z)} \right] + \frac{1}{2(\Omega_0 - 1)} \left[1 - \frac{(1 + \Omega_0 z)^{1/2}}{(1+z)^2} \right]. \end{aligned} \quad (7.113)$$

If $\Omega_0 < 1$, the inverse trigonometric functions are replaced by inverse hyperbolic functions according to the rule $\sin^{-1} ix = i \sinh^{-1} x$.

The $\theta - z$ relation (7.112) is compared with the standard result (7.104) in Fig. 7.13. It can be seen that the minimum in the standard $\theta - z$ relation disappears in the maximally inhomogeneous model. Thus, if no minimum is observed in the $\theta - z$ relation for a class of standard rods, it does not necessarily mean that the Universe must have $\Omega_0 \approx 0$. It might just mean that the Universe is of high density and is highly inhomogeneous.

Dyer and Roeder have presented the analytic results for intermediate cases in which a certain fraction of the total mass density is uniformly distributed within the light cone (Dyer and Roeder, 1973). A particularly simple result is found for the case of the Einstein–de Sitter model in which it is assumed that a fraction α of the total mass density is uniformly distributed within the light cone, the remainder being condensed into discrete point masses. It is assumed that the light cone does not pass so close to any of the point masses that strong gravitational lensing distorts the light

cones. They find the simple result:

$$L = \Theta D_A = \Theta \frac{2}{\beta} (1+z)^{(\beta-5)/4} [1 - (1+z)^{-\beta/2}], \quad (7.114)$$

where $\beta = (25 - 24\alpha)^{1/2}$. It can be seen that (7.114) reduces to (7.104) and (7.112) in the limits $\alpha = 1$ and $\alpha = 0$ respectively. The angular diameter–redshift relation for the case $\alpha = 0.5$ is included in Fig. 7.13. Finding the minimum of (7.114), Dyer and Roeder also show that, for the Einstein–de Sitter model, the minimum in the angular diameter–redshift relation occurs at a redshift (Dyer and Roeder, 1973),

$$\alpha = 1. \quad z_{\min} = \left(\frac{5+\beta}{5-\beta} \right)^{2/\beta} - 1. \quad (7.115)$$

Thus, if a minimum is observed in the $\theta - z$ relation, there must be matter within the light cone and limits can be set to the inhomogeneity of the matter distribution in the Universe. The effects upon the observed intensities of sources may be evaluated using the same approach as in Sect. 7.4.5. The $\theta - z$ relation may be used to work out the fraction of the total luminosity of the source incident upon the observer's telescope using the reciprocity theorem. The end results are not so very different from those of the standard models.

The case of strong gravitational lensing, in which the light cone subtended by the source at the observer passes close to a massive deflector, was discussed in Sect. 4.6. As shown in that section, strong gravitational lensing causes major distortions of the images of distant background sources, if they lie within roughly the Einstein angle θ_E , given by (4.42) and (4.63), of the deflector. The types of distortion, illustrated in Fig. 4.20, have been observed in a number of gravitationally lensed sources in the optical and radio wavebands. In addition, the flux densities of the background sources can be enhanced by factors of up to about 40 over their unlensed intensities. This type of flux density enhancement has been shown to account for the extraordinary luminosity of the galaxy IRAS F10214+4724. Assuming the galaxy were unlensed, its far-infrared luminosity would be $\sim 3 \times 10^{14} L_\odot$. The image of the galaxy is, however, clearly distorted because of strong gravitational lensing and, once a best-fitting mass model has been used to determine the flux density enhancement, the far-infrared luminosity of the galaxy is found to be $\sim 10^{13} L_\odot$, still a very large value, but not as extreme as once believed (Close et al., 1995).

As mentioned in Sect. 4.6, even in the weak lensing limit, the images of background objects are distorted by the presence of mass concentrations along the line of sight. These distortions are often referred to as the effects of *cosmic shear* upon the images of galaxies and can be used to determine the distribution of dark matter in the intervening objects. An example of this technique for determining the distribution of dark matter in the rich cluster of galaxies Cl 0024+1654 was shown in Fig. 4.21.

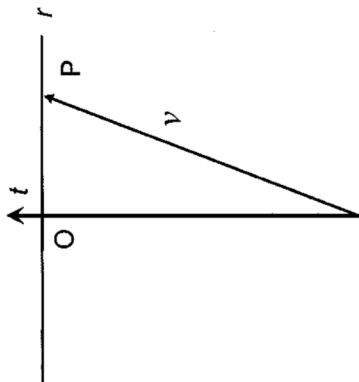
Kaiser has also shown how the statistics of the distortions of background objects by intervening mass concentrations can be used to determine the power spectrum of density fluctuations in the large-scale distribution of matter in the Universe (Kaiser, 1992). We will return to this topic in Sect. 15.8.5.

A7 The Robertson–Walker Metric for an Empty Universe

The world model containing no matter at all, $\Omega_0 = 0, \Omega_A = 0$, is often referred to as the *Milne model*. We have already emphasised the contradictions inherent in using the special theory of relativity in the presence of gravitational fields. In this special case, however, there are no gravitational forces since there is no matter present.

The value of this analysis is that it brings out the importance of the cosmological principle in the setting up of the framework for cosmological models. We will show how the appropriate Robertson–Walker metric can be derived for this special case. In the empty model, test particles move apart at constant velocity from $t = 0$ to $t = \infty$. The origin of the uniform expansion is taken to be $[0, 0, 0, 0]$ and the world lines of particles diverge from this point, each point maintaining constant velocity with respect to the others. The space–time diagram for this case is shown in Fig. A7.1, our own world line being the t axis and that of particle P having constant velocity v with respect to us.

The problem becomes apparent as soon as we attempt to define a suitable *cosmic time* for ourselves and for a fundamental observer moving with the particle P . At time t , the observer P is at distance r and, since v is constant, $r = vt$. Because of the



$[0,0,0]$

Fig. A7.1. The space–time diagram for an empty Universe

relativity of simultaneity, however, the observer P measures a different time τ from the observer O . From the Lorentz transformation,

$$\tau = \gamma \left(t - \frac{vr}{c^2} \right); \quad \gamma = \left(1 - \frac{v^2}{c^2} \right)^{-1/2}.$$

Since $r = vt$,

$$\tau = t \left(1 - \frac{r^2}{c^2 t^2} \right)^{1/2}. \quad (\text{A7.1})$$

The problem is that t is only proper time for the observer at O and for nobody else. We need to be able to define surfaces of constant cosmic time τ , because it is only on these surfaces that we can impose conditions of isotropy and homogeneity on the large-scale structure of the Universe, in accordance with the cosmological principle. Therefore, the surface of constant cosmic time τ is

$$\tau = t \left(1 - \frac{r^2}{c^2 t^2} \right)^{1/2} = \text{constant}. \quad (\text{A7.2})$$

Locally, at each point in the space, this surface must be normal to the world line of the fundamental observer.

Next we define the element of radial distance dl at the point P on the surface $\tau = \text{constant}$. The interval $ds^2 = dr^2 - (1/c^2) dr^2$ is an invariant. Over the $\tau = \text{constant}$ surface, $ds^2 = -(1/c^2) dl^2$ and hence

$$dl^2 = dr^2 - c^2 dr^2. \quad (\text{A7.3})$$

τ and dl define locally the proper time and proper distance of events at P and are exactly the elements cosmic time t and radial distance coordinate x introduced in Sects. 5.1 and 5.4. This analysis clarifies why the metric of empty space is not a simple Euclidean metric.

Let us now transform from the frame S to the frame S' at P moving at radial velocity v . Distances perpendicular to the radial coordinate remain unaltered under Lorentz transformation and therefore, if in S ,

$$ds^2 = dt^2 - \frac{1}{c^2} dr^2 + r^2 d\theta^2, \quad (\text{A7.4})$$

the invariance of ds^2 means that

$$dt^2 - \frac{1}{c^2} dr^2 = d\tau^2 - \frac{1}{c^2} dl^2, \quad (\text{A7.5})$$

the perpendicular distance increment $r^2 d\theta^2$ remaining unaltered. Therefore, in S' ,

$$ds^2 = d\tau^2 - \frac{1}{c^2} (dl^2 + r^2 d\theta^2). \quad (\text{A7.6})$$

Now we need to express r in terms of l and τ to complete the transformation to the (τ, l) coordinate system.

Along the surface of constant τ ,

$$dl^2 = dr^2 - c^2 dr^2. \quad (\text{A7.7})$$

The Lorentz transform of $d\tau$ is

$$d\tau = \gamma \left(dr - \frac{v}{c^2} dr \right) = 0,$$

and hence,

$$dr^2 = \frac{v^2}{c^4} dr^2, \quad (\text{A7.8})$$

that is, from (A7.7)

$$dl^2 = dr^2 \left(1 - \frac{v^2}{c^2} \right) = dr^2 \left(1 - \frac{r^2}{c^2 l^2} \right). \quad (\text{A7.9})$$

Hence we need only replace l by τ using (A7.1) to find a differential expression for dr in terms of dl and τ ,

$$dl = \frac{dr}{\left(1 + \frac{r^2}{c^2 \tau^2} \right)^{1/2}}. \quad (\text{A7.10})$$

Integrating using the substitution $r = c\tau \sinh x$, the solution is

$$r = c\tau \sinh(l/c\tau). \quad (\text{A7.11})$$

The metric (A7.6) can therefore be written

$$ds^2 = dr^2 - \frac{1}{c^2} [dl^2 + c^2 \tau^2 \sinh^2(l/c\tau) dl^2]. \quad (\text{A7.12})$$

This corresponds precisely to the Robertson–Walker metric for an empty Universe. The geometry is an isotropic curved space with hyperbolic geometry, the radius of curvature of the geometry \mathcal{N} being $c\tau$. This explains why an empty universe has hyperbolic spatial sections. The conditions (A7.1) and (A7.10) are the key relations which indicate why we can only define a consistent cosmic time and radial distance coordinate in hyperbolic rather than flat space.